



Effects of coal mining on the evolution of groundwater hydrogeochemistry

Wei Qiao^{1,2} · Wenping Li^{1,2} · Shengcai Zhang³ · Yunfei Niu⁴

Received: 29 October 2018 / Accepted: 25 March 2019 / Published online: 15 April 2019
© Springer-Verlag GmbH Germany, part of Springer Nature 2019

Abstract

The mining industry, especially coal mining, may severely affect the spatial and temporal evolution of groundwater. To provide a potential model outlining the hydrogeochemical evolution of groundwater as influenced by coal mining, a multi-layer groundwater system in a coal mining area was investigated. A total of 76 groundwater samples were collected between 1964 and 2018 for hydrogeochemical analysis from boreholes, underground tunnels, and surface pits at Xinglongzhuang Coal Mine in China. Hierarchical cluster analysis and principal component analysis were used to classify four significant groundwater zones and two principal components. The results showed that mining may have caused the rock strata to sink, obstructing the path linking the Permian and lower Quaternary aquifers, and resulting in intensified ion exchange in the lower Quaternary aquifer. The concentrations of Na^+ and Ca^{2+} in the groundwater from the lower Quaternary aquifer changed over the studied period (~54 years). The gradual increase of Na^+ and decrease of Ca^{2+} concentration verified the action of cation exchange. The four main aquifers had relatively independent hydrogeochemistry, suggesting that the hydraulic conductivity of the natural faults is weak and the sealing properties of hydrogeological drill holes in the coal field are good. Analysis of 26 heavy metals in the mine drainage water showed that there is only minor pollution after the water has been simply treated. These data analysis methods and results could be useful in areas with long-term mining to interpret the evolution of groundwater and to promote groundwater quality management.

Keywords Groundwater monitoring · Hydrogeochemistry · Mining · Multivariate statistics · China

Introduction

Throughout China, coal mining is crucial to the Chinese economy, accounting for 61.8% of the country's primary energy consumption in 2016, and is expected to remain at similar levels until at least 2020. Meanwhile, groundwater is often the preferred source of water supply as it tends to be a more reliable and economically viable resource than surface water, and more resilient to pollution. Unfortunately, coal mining and groundwater resource management frequently come into conflict, and the detrimental effects of coal mining on water resources has been well documented globally (Adam and Paul 2000; Andreas and Nikola 2011; Johnson and Younger 2006). Mine safety is a main issue, as the potential inrush of groundwater at the working face or tunnel face during the mining of deep coal seams poses a serious threat to both miners and their operations (Zhang 2005). China has a long history of mining disasters and the Chinese government is well aware of the dangers, but given that the Chinese economy is highly dependent on its coal resources, the challenge has been to develop

✉ Wei Qiao
qiaowei@cumt.edu.cn

✉ Wenping Li
wpli@cumt.edu.cn

¹ Institute of Mine Water Hazards Prevention and Controlling Technology, China University of Mining and Technology, 1 Daxue Road, Xuzhou, Jiangsu 221116, People's Republic of China

² School of Resources and Geosciences, China University of Mining and Technology, 1 Daxue Road, Xuzhou, Jiangsu 221116, People's Republic of China

³ Xingloanzhuang Coal Mine, Yanzhou Coal Mining Company Limited, Yankuang Group, Xinglongzhuang Town, Jining, Shandong 272102, People's Republic of China

⁴ Beijing Exploration Resources Technology Co., 1002 C# Yingkunshiji, Science Park, Fengtai, Beijing 100166, People's Republic of China

ways of mitigating and managing risk while ensuring coal production targets are maintained. Overlying aquifers, which are aquifers above the coal seam, are the main source of intruding water that can enter through mining fractures, faults, or pores (Wu et al. 2014). Overlying-aquifer water inrush is the most common and dangerous threat to coal mine workers. Wu et al. (2014) reported that in Jurassic and Permian overburden strata, overlying aquifers are generally sandstone, whereas in Carboniferous strata they are limestone and sandstone. The overburden strata, located above the coal seam and the goaf, are generally classified into three distinct zones: the caved zone, the fractured zone and the continuous deformation zone. If an overlying aquifer is crossed by the caved or fractured zone, groundwater would rush into the mining spaces or gobs.

Overlying-aquifer water disasters at coal mines are widespread and have been a major threat to both coal mining and the environment. Pumping can alleviate this risk, but this can lead to secondary issues such as land subsidence, mine collapse, and the unnatural inducement of water from neighboring water-resource aquifers and even the ground surface (Unlu et al. 2013; Salmi et al. 2017; Qiao et al. 2017). The hydrogeological environment is always altered by mining activities, mainly due to the drainage of the aquifer, which results in the formation of a cone of depression and the reduction of available groundwater resources. Han et al. (2013) reported the characteristics of hydrogeochemical evolution in Ordovician limestone groundwater in the Yanzhou coal mining area, North China. Li et al. (2018) evaluated the water quality status and associated hydrochemical groundwater processes at a phosphorite mine in China. Rakotondrabe et al. (2018) analyzed the influence of goldmining activities on the water quality in the Mari catchment in Bétaré-Oya (East Cameroon), and tested for the trace elements Pb, Cd, Mn, Cr, and Fe, which were found to be at concentrations unsuitable for human consumption. Razowska (2001) reported changes in groundwater chemistry caused by the flooding of iron mines in the Czeszochowa Region, southern Poland, and found that 15 years after the flooding, water stored in the working mine may be defined as quasi-stagnant, while Middle Jurassic aquifer water supplies located in Czeszochowa are not polluted by mine waters today. Babita et al. (2017) investigated major and trace element geochemistry of the coal mine water in the North Karanpura coalfields in India. Bhattacharya et al. (2012) investigated groundwater chemistry with special attention to metal pollution in selected communities in the Wassa West district, Ghana, and proposed that the aquifers are not strongly affected by weathering of minerals due to short groundwater residence times and intense flushing.

The hydrogeochemical evolution of groundwater has been extensively investigated, concentrating on water–rock interactions as the main mechanism. Various methods including

multivariate statistical analysis, isotopes analysis, and hydrogeochemical modeling have been employed to interpret the complex processes (Plummer et al. 1990; Güler et al. 2002; Sharif et al. 2008; Carucci et al. 2012; Voutsis et al. 2015; Cortes et al. 2016). Investigators have reported comparable issues in coal mining areas of China. Methods such as analysis of groundwater ions, trace elements and environmental isotopes, and tracer tests, have been employed to explore the origins and flow characteristics of aquifers in North China coalfields (Guo et al. 2003; Chen et al. 2013; Huang et al. 2016).

In China, the overlying aquifer for Jurassic and Permian coal formations consists of mainly shallow, sandy, confined sandstone systems. In eastern China, the Permian coal seams are the major mining targets, and as a result, the Permian sandstone aquifer above the coal seams is the drainage source such as the porous and fractured sandstone aquifer in the Shanxi Group of the Permian System. In western China, the primary mineable coal seams are distributed in a Jurassic system, so that most of the water in the mine enters through the porous and fractured sandstone or conglomerate aquifer in Jurassic and Cretaceous systems such as the Yan'an and Zhiluo groups (Jurassic) or Yijun and Luohe groups (Cretaceous). In coal mining areas in northwest China, there is a stable layer of confined aquifer, such as the Salawusu Group in the Quaternary system, which is in a shallow position and plays an important role in surface ecology. The Xinglongzhuang Coal Mine was the focus of this investigation, and is a typical North China Coal Mine. Groundwater at this mining site is not only a resource, but also threatens the safety of miners and the mining operation. The primary concern of residents in the area is the impact of long-term coal mining on groundwater connections and quality.

The Xinglongzhuang Coal Mine, part of the Yanzhou coal field in Shandong Province, eastern China, was used as a case study to assess the hydrogeochemistry and main hydraulic connections of the groundwater system. The potential water–rock interactions were evaluated to interpret the hydrogeochemical evolution of the upper Quaternary, lower Quaternary, Permian, and Ordovician groundwater at the Xinglongzhuang Coal Mine in North China. The spatial and temporal variations of major cations, anions, and trace elements were analyzed to explain the evolution of the groundwater, and to provide a better understanding of the mine-water environment, hydroconductivity of geological structures, and mine drainage effect, and to advance the strategic management of groundwater resources in the mining area.

Study Area

The study focused on the Xinglongzhuang Coal Mine, part of the Yanzhou coal field in Shandong Province,

eastern China (Fig. 1). The surface of the study area is a relatively flat, Quaternary alluvial plane at an elevation of between 44 and 52 m above sea level (masl). Average annual precipitation is 714 mm and the mean annual air temperature is 14.4 °C. The Xinglongzhuang Coal Mine has an area of 57.7 km². Until recently, mining operations focused on the No. 3 coal seam, which had an average thickness of 8 m (recorded in 1981). The No. 3 coal seam was extracted using fully mechanized caving technology, and has been approved to produce approximately 6–7 million tonnes of coal per year since 2000.

Below the alluvium, Mesozoic and Paleozoic sedimentary formations form a shallow syncline (limb dip angles of <10°) that plunges gently towards the southeast. The

Xinglongzhuang Coal Mine is located at the north wing of the Yanzhou Syncline. Generally, it is a cambered monoclinical structure with sub-folds developed along with some faults. Under the influence of the sub-folds including a Juwanglin anticline, Dashicun syncline, and Damiao anticline, the cambered monoclinical structure extrudes slightly to the east. The Ziyang and Puzi Faults are located at the east and west borders, respectively, and the Juwanglin anticline stretches across the middle part of the mine, controlling the tendency of strata.

The full sedimentary sequence for the study area is shown in Fig. 2. Aquifers that could negatively influence operations in the coal mine may include: overlying aquifers in the Permian sandstones and surficial sands and gravels of the Quaternary, and the thick-bedded Ordovician karst aquifer. There are two aquifer groups in the Quaternary formation.

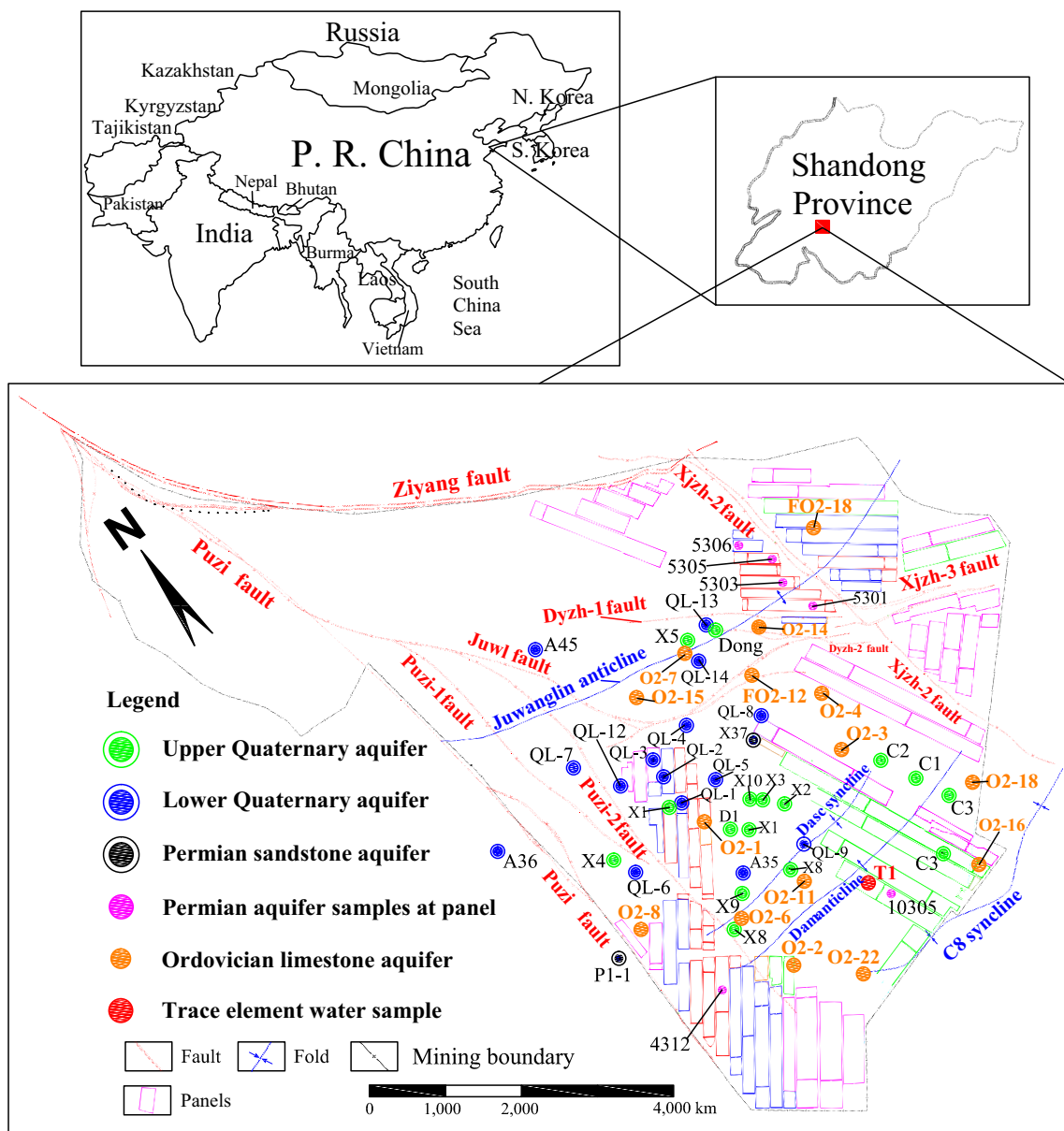


Fig. 1 General map of the studied area and water samples locations

Fig. 2 Stratigraphic column of the study area

Epoch	Thickness(m) Range Average	Lithology
Quaternary	18.47 to 225.29 136.30	Clay, sand, gravel
Upper Jurassic	0 to 794.86	Fine sandstone, mudstone
Middle Permian	0 to 79.90	Mudstone, sandy mudstone
	0 to 181.88 60.00	Aluminum mudstone, fine sandstone
Lower Permian	0 to 152.91 117.26	Fine-medium sandstone, mudstone, coal
Upper Carboniferous -Middle Permian	148.53 to 218.00 172.60	Siltstone, limestone, mudstone, coal
Upper Carboniferous	18.42 to 86.69 43.00	Limestone, clay rock, mudstone
Middle Ordovician	65.00 to 121.00 90.14	Micritic limestone, micritic dolomite limestone
	105.00 to 127.00 111.49	Micritic dolomite limestone, lime dolomite
Lower Ordovician	202.00 to 227.00 206.66	Micritic limestone, dolomite limestone
	198.00 to 282.00 212.00	Marl, micritic limestone, mud dolomite
	86.00 to 117.00 110.00	Dolomite limestone, lime dolomite

The upper group has an average thickness of 54.54 m, and is comprised of clay, sandy clay, loose quartz sand, and gravel layers with inter-deposition of aquiclude layers. The lower gravel aquifer in the Quaternary formation is distributed in the western and northern parts of the Xinglongzhuang Coal Mine with an average thickness of 38.87 m. The upper and lower aquifer groups have only tenuous hydraulic contact. Precipitation recharges the upper aquifer groups, which in turn recharge the lower groups. The lower gravel aquifer is an indirect water resource which could recharge the Permian sandstones. The Permian porous and fractured sandstone aquifer has a thickness of 3.28–41.73 m with an average value of 13.08 m, and is the aquifer that causes the direct water-inrush during the mining of the No. 3 coal seam. Carbonates of the Middle Ordovician Badou group are comprised of grey limestones or grey dolomites with a massive, compact structure and an average thickness of 530 m. Where the hydraulic conductivity of the aquitard is enhanced by fractures, flows could lead to very rapid and severe flooding of the coalface and mine workings as the excavation proceeds. Because of these issues, this report concentrates on investigating the hydraulic connections and hydrogeochemical evolution of the groundwater from the Quaternary, Permian, and Ordovician aquifers.

Materials and methods

Sample collection and analysis

For this study, 72 water samples comprised of groundwater, tunnel water, and surface pit water, were obtained from the study area and analyzed for water quality. Surface pit water is obtained when, occasionally, a surface pit collapses due to mining, resulting in the mine groundwater being discharged. The data were taken from 1964 to 2018, and included 17 samples from the upper Quaternary (QU) aquifer, 16 samples from the lower Quaternary aquifer (QL), 16 samples from the Permian sandstone aquifer (P), 14 samples from the Ordovician limestone aquifer (O2), and 9 samples from ditches in underground tunnels (Pit) collected from the Mine Geological Report for the Xinglongzhuang Coal Mine for analysis (Table 1). In addition, five samples from panels, ditches, and surface pits were collected and tested in June 2017 for trace elements analyses. The locations of these samples are displayed in Fig. 1.

All the samples were collected using polyolefin bottles. The containers were washed four or five times using the water to be sampled before the sample was taken. The bottles were

Table 1 General statistics of groundwater samples, tunnel water and surface pit water. All indices are expressed in mg/L except pH

No.	Sample location	Label	Year	pH	Na	Ca	Mg	Cl	SO4	HCO ₃	Type	Fe ³⁺	NH ₄ ⁺	NO ₃ ⁻	NO ₂ ⁻	TDS	TH
1	Permian sandstone aquifer	P-4311	1981	8.1	288.21	4.61	1.8	47.94	14.2	652.73	Na-HCO ₃	0	0.004	0	0.01	1,009.50	18.92
2		P-5303	1981	8.4	242.26	1.36	0.33	28.58	10.08	520.56	Na-HCO ₃	0	0	0	0.01	803.18	48.01
3		P-2307	1983	8.2	182.87	4.67	9.76	42.74	2.26	473.25	Na-HCO ₃	0.02	0.36	0	0	715.93	51.76
4		P-5300	1983	8.2	222.46	3.37	0.88	31.43	20.37	507.55	Na-HCO ₃	0.02	0	0.5	0.23	786.81	11.96
5		P-2304	1984	7.9	132.92	7.98	0.91	44.43	16.46	284.1	Na-HCO ₃	0	0	0	0	486.80	23.72
6		P-4312	1988	7.7	560.45	35.33	24.55	179.34	316.44	1,010.47	Na-HCO ₃	0.5	0.58	0	0	2,127.66	189.17
7		P-5302	1988	8.1	314.11	16.73	4.51	46.84	48.97	700.01	Na-HCO ₃	0.08	0.04	0	0	1,131.29	60.33
8		P-5301	1988	7.9	227.33	18.6	6.49	37.87	62.14	547.71	Na-HCO ₃	0.02	0.02	0.62	0.01	900.81	73.17
9		P-5306	1992	7.9	358.39	17.82	6.14	118.4	202.51	275.05	Na-HCO ₃	0.08	0	0	0	978.39	24.82
10		P-1301	1994	7.7	237.38	10.22	3.58	44.53	90.55	487.31	Na-HCO ₃	0.04	0	0	0	873.61	40.24
11		P-2304	1995	8.1	156.01	58.98	11.2	42.3	62.5	514.95	NaCa-HCO ₃	0	0	0.27	0	846.21	193.30
12		P-5301	1999	8.1	264.55	49.09	14.29	35.16	73.66	746.47	Na-HCO ₃	0.04	0	0	0	1,183.26	181.40
13		P-5305	1999	7.9	456.33	29.53	8.48	39.35	152.09	1,045.88	Na-HCO ₃	0.58	0.28	0	0	1,732.52	108.70
14		P-4314	2000	8.1	332	41.67	12.9	40.04	237.43	656.59	Na-HCO ₃ -SO ₄	0.28	0.1	0	0	1,321.01	157.10
15		P-4-m	2000	7.6	312.7	55.7	11.35	40.87	204.82	688.46	Na-HCO ₃	0.07	0.15	0.09	0	1,314.21	185.80
16		P-P1-1	2010	8.4	79.53	11.3	5.43	44.46	40.33	118.04	Na-HCO ₃	0.6	0.02	0	0	299.71	50.51
17	Upper Quaternary aquifer	QU-C1	1978	7.7	17.55	61.14	8.62	14.18	12.35	234.92	Ca-HCO ₃	0	0	1.07	0	349.83	232.71
18		QU-C2	1979	7.8	10.1	57.96	13.78	9.79	11.11	241.03	Ca-HCO ₃	0	0.1	0.89	0	344.76	227.74
19		QU-C3	1985	7.6	18.84	70.04	14.06	7.84	7	310.46	Ca-HCO ₃	0.02	0	0.89	0.07	429.22	239.17
20		QU-X1	1982	7.3	11.39	71.38	12	29.78	53.91	183.8	Ca-HCO ₃	0.04	0	4.5	0.02	366.82	190.42
21		QU-X2	1983	7.9	27.19	71.59	14.68	20.56	19.96	301.37	Ca-HCO ₃	0.04	0.01	1.5	0.33	457.23	208.64
22		QU-X3	1983	7.9	30.06	59.74	10	11.31	18.93	250.64	CaNa-HCO ₃	0.02	0	18	0.03	398.73	211.14
23		QU-X4	1979	7.6	22.01	60.86	13.77	14.68	9.88	247.28	Ca-HCO ₃	0.04	0	0.89	0	369.41	202.22
24		QU-X5	1979	7.7	18.81	69.06	9.39	22.52	18.93	244.14	Ca-HCO ₃	0.02	0	0	0.02	382.89	179.91
25		QU-X6	1987	7.4	34.66	64.52	9.99	32.66	42.18	226.38	CaNa-HCO ₃	0.02	0.02	2.6	0.07	413.10	222.21
26		QU-X7	1987	7.6	41.93	48.51	14.28	19.28	35.39	252.26	CaNa-HCO ₃	0.02	0	0.2	0.07	404.73	336.43
27		QU-X8	1990	7.7	22.45	64.11	15.08	27.9	27.57	247.55	Ca-HCO ₃	0.06	0	0	0.01	411.94	232.71
28		QU-X9	1991	7.7	39.08	102.89	19.3	51.8	96.29	301.98	Ca-HCO ₃	0.08	0	0.53	0.01	611.96	176.71
29		QU-X10	1988	7.3	14.05	61.73	19.09	8.93	28.81	265.19	Ca-HCO ₃	0.02	0	4	0.01	401.83	158.84
30	QU-D1	1990	7.8	16.23	55.23	9.34	8.59	5.35	230.51	Ca-HCO ₃	0	0	3.07	0.56	328.88	216.84	
31	QU-EG	1997	7.8	44.18	52.24	6.91	14.82	26.34	251.89	CaNa-HCO ₃	0.14	0	0.44	0.16	397.12	195.97	
32	QU-G	1984	7.3	28.01	71.36	9.39	20.92	12.35	287.03	CaNa-HCO ₃	0	0	0	0	429.06	232.71	
33	QU-Ch	1981	7.6	18.4	63.85	8.86	13.83	20.16	235.17	Ca-HCO ₃	0.02	0.02	3.32	0.01	363.64	227.74	
34	Lower Quaternary aquifer	QL-A45	1964	7.5	76.15	64.05	9.58	149.78	25.67	63.37	NaCa-Cl-HCO ₃	0	0	0	0	388.60	193.36
35		QL-A35	1968	7.7	65.02	48.06	13.38	126.46	34.18	32.92	NaCa-Cl	0	0	0	0.53	320.55	175.09
36		QL-2	1968	7.5	23.94	70.07	11.34	40.8	63.37	171.47	Ca-HCO ₃	0.04	0.04	12	0.07	393.14	221.65
37		QL-3	1989	7.8	56.28	37.89	9.44	35.94	46.29	188.61	NaCa-HCO ₃	0	0.02	3	0	377.47	133.52
38		QL-5	1991	7.7	37.08	19.2	9.44	44.2	15.84	109.74	NaCa-HCO ₃ -Cl	0.02	0.48	0	0	236.00	86.92
39		QL-6	1994	8.6	74.08	21.8	11.96	123.86	6.38	82.3	Na-Cl-HCO ₃	0.02	0.34	0	0	320.74	103.7
40		QL-7	1996	7.7	33.6	67.43	9.22	10.42	28.39	287.04	CaNa-HCO ₃	0.04	0.04	0	0.03	436.21	206.34
41		QL-G2	1998	8.2	54.4	64.19	15.17	46.38	47.73	263.59	CaNa-HCO ₃	0.02	0	0.5	0	491.98	222.75
42		QL-8	2000	7.6	41.93	48.51	14.28	19.28	35.39	252.26	CaNa-HCO ₃	0.02	0	0.2	0.07	411.94	179.91
43		QL-C5	2003	7.9	54.42	47.53	9.29	29.67	27.57	250.12	NaCa-HCO ₃	0.14	0	0	0	418.74	157.04
44		QL-13	2006	7.8	48.48	43.82	5.94	12.56	20.39	255.3	NaCa-HCO ₃	0.04	0	0	0	386.53	133.81

Table 1 (continued)

No.	Sample location	Label	Year	pH	Na	Ca	Mg	Cl	SO ₄	HCO ₃	Type	Fe ³⁺	NH ₄ ⁺	NO ₃ ⁻	NO ₂ ⁻	TDS	TH
45		QL-SG1	2009	7.9	64.84	54.99	9.29	39.56	49.38	256.1	NaCa-HCO ₃	0.4	0	0.44	0	475.00	175.61
46		QL-SG2	2011	7.9	84.13	58.92	10.48	40.55	92.59	268	NaCa-HCO ₃	0.34	0	0.71	0.16	555.88	190.27
47		QL-ZF	2014	7.8	60.22	54.33	9.17	30.41	33.29	267.71	NaCa-HCO ₃	0	0	1	0	456.13	173.46
45		QL-9	2016	7.2	108.35	37.68	11.42	38.96	65.84	304	Na-HCO ₃	0.06	0.02	4	0.86	571.19	141.48
49		QL-12	2018	8	87.7	39.68	7.15	36.58	69.96	238.22	NaCa-HCO ₃	0	0	0.44	0.07	479.80	128.52
50	Ordovician Limestone aquifer	O2-1	2005	7.7	44.8	333.36	94.36	35.88	1,024.79	230.15	Ca-SO ₄	0.6	0.1	0.33	<0.008	1,764.37	1,220.91
51		O2-2	2005	7.8	63.82	368.55	100.45	44.05	1,121.52	240.11	Ca-SO ₄	5	<0.04	3.72	<0.008	1,947.64	1,333.89
52		O2-3	2005	7.4	70.13	304.37	86.64	49.05	932.94	243.84	Ca-SO ₄	2	<0.04	1.47	<0.008	1,690.44	1,116.75
53		O2-4	2005	7.3	46.26	277.45	79.11	53.62	796.97	241.35	Ca-SO ₄	3	<0.04	13.41	<0.008	1,511.17	1,018.52
54		O2-6	2006	7.8	54.66	371.17	108.08	42.62	1,178.61	212.38	Ca-SO ₄	0.5	<0.04	0.2	<0.008	1,968.22	1,371.81
55		O2-7	2006	7.5	31.82	218.86	66.63	21.87	661.56	198.93	CaMg-SO ₄	<0.08	<0.04	0.2	<0.008	1,199.87	820.85
56		O2-8	2006	7.7	62.46	259.06	139.23	45.67	1,076.92	159.95	CaMg-SO ₄	0.5	0.8	0.13	<0.008	1,744.72	1,220.13
57		O2-11	2006	7.7	62.26	327.41	121.78	47.07	1,165.56	208.34	Ca-SO ₄	0.2	0.15	<0.1	<0.02	1,932.77	1,318.99
58		O2-15	2006	7.2	26.96	193.56	54.78	20.45	537.11	256.38	Ca-SO ₄ -HCO ₃	1	<0.04	0.13	<0.008	1,090.37	708.88
59		O2-14	2011	7.3	123.68	197.83	54.1	45.41	660.06	299.68	CaNa-SO ₄ -HCO ₃	0.5	<0.04	0.04	<0.008	1,381.30	812.93
60	O2-F18	2011	7.6	63.99	327.95	92.81	44.19	1,095.63	243.33	Ca-SO ₄	0.25	<0.04	0.24	<0.008	1,868.39	1,201.04	
61	O2-22	2011	7.8	19.95	145.09	47.49	12.68	352.51	256.14	Ca-SO ₄ -HCO ₃	0.65	0.06	1.09	0.01	835.67	557.84	
62	O2-18	2012	7.6	111	252.72	76.63	47.03	841.14	284.12	CaNa-SO ₄	1.25	0.25	0.04	<0.008	1,614.18	946.57	
63	O2-F12	2011	7.6	49.22	213.34	72.22	48.28	657.28	262.54	Ca-SO ₄ -HCO ₃	0.15	<0.04	0.08	<0.008	1,303.11	830.07	
64	Tunnel water	T-cen	1985	8.3	295.27	11.06	5.19	56.87	165.42	442.2	Na-HCO ₃	0.12	0.3	0	0	976.46	49.09
65		T-east	1985	8.3	296.31	9.36	5.62	62.12	179	401.75	Na-HCO ₃	0.3	0.3	0	0	954.76	46.4
66		T-sub	1985	8.7	282.07	10.56	3.66	51.16	57.2	513.47	Na-HCO ₃	0.3	0	0	3.62	922.04	41.39
67		T-west	1985	7.7	148.35	49.8	29.91	127.01	151.84	280.93	Na-HCO ₃ -SO ₄	0.04	0	0	2.3	790.18	247.57
68		T-pan	2017	7.98	4.34	36.15	20.72	49.63	52.68	405.72	CaMg-HCO ₃	0.11	0	0	0	569.35	-
69		T-dit	2017	8.48	5.07	14.06	19.49	69.49	206.62	815.41	MgCa-HCO ₃	0.05	0	0.1	0	1,130.29	-
70		T-Ordo	2017	7.91	7.61	160.72	57.99	49.63	551.96	314.74	CaMg-SO ₄ -HCO ₃	0.06	0	0.11	0	1,142.82	-
71	T-sum	2017	7.93	7.84	104.47	68.22	54.14	466.34	428.67	CaMg-SO ₄ -HCO ₃	0.08	0	0.09	0	1,129.85	-	
72	Surface pit water	T-pit	2017	8.12	8.75	63.49	45.56	139.86	438.35	607.03	CaMg-HCO ₃ -SO ₄	0.08	0	0.14	0	1,303.26	-

sealed immediately and then transported to the laboratory for physicochemical analysis. Some of the samples were analyzed for total dissolved solids (TDS), total hardness (TH), pH, major cations (Na^+ , K^+ , Ca^{2+} , Mg^{2+}) and major anions (SO_4^{2-} , Cl^- , HCO_3^-).

Traditional titrimetric methods were used to determine the concentrations of SO_4^{2-} , Cl^- , and HCO_3^- , while the EDTA titrimetric method was used for cation analysis of Ca^{2+} , Mg^{2+} , and TH. Na^+ and K^+ were tested using flame atomic absorption spectrometry. The accuracies of analyses for all samples were based on measurements calculating the ionic balance error, which was assigned an upper error limit of 4%. All sample errors were below the upper limit value. All analyses were performed in the laboratory of the Geological Engineering Survey Institute of South Shandong using standard procedures recommended by the Chinese Ministry of Land and Resources (CMLR). Stable isotopic compositions were also conducted for selected samples using a Finnigan MAT 253 isotope ratio mass spectrometer at the China University of Mining and Technology. Concentrations of trace metals in water samples from the Xinglongzhuang Coal Mine were detected by ICP-MS (Perkin Elmer) at the Jiangsu Design and Research Institute of Geology and Mineral resources, Xuzhou, China.

Multivariate techniques

Hierarchical cluster analysis (HCA) and principal component analysis (PCA) are the most popular methods for statistical analysis of multidimensional and complex systems, and have been employed in many similar studies (Blake et al. 2015; Sako et al. 2016; Chihi et al. 2015). As in other similar research, R-mode HCA was used in this study to better understand the origin of or the factors influencing the hydrochemistry. Principal component analysis (PCA) is frequently used to reduce the dimensionality of data and to create new uncorrelated components (Güler et al. 2002; Voutsis et al. 2015; Morán-Ramírez et al. 2016). The results of PCA are usually discussed in terms of factor scores and loadings. In this study, PCA was used for hydrogeochemical data analysis.

Results and discussion

General hydrogeochemical properties

Hydrogeochemistry depends on many factors including the hydrogeological settings, lithology, mineral composition, temperature, climate, relationship between adjacent aquifers, and presence of mining and other human activities (Li et al. 2017; Towfiqul Islam et al. 2017). To help explore the general water chemistry of the groundwater in the study area, the statistical

summary of hydrogeochemical values is presented in Table 1. There are a total of 72 groundwater samples, comprised of 16 samples from the Permian sandstone confined aquifer above coal seam 3 (from 1981 to 2010), 17 samples from the upper Quaternary confined aquifer (from 1978 to 1997), 16 samples from the lower Quaternary confined aquifer (from 1980 to 2018), 14 samples from the Ordovician limestone aquifer (from 2005 to 2012), and 9 samples from underground tunnels and surface pits (from 1985 to 2017).

As shown in Table 1, the pH of all the water samples ranges from 7.2 to 8.7, with average values of 8.02 for P, 7.63 for QU, 7.8 for QL, 7.57 for O2, 8.16 for T, and 8.12 for Pit, which means the water was generally slightly (7.2) to moderately (8.7) alkaline. Due to the tunnel water mostly coming from the Permian aquifer, the groundwater had a more alkaline environment in this area. The TDS of groundwater from the four main aquifers ranged from 236.00 to 2,129.66 mg/L. Arranged in descending order of TDS, the results indicate that the water–rock interaction increased with depth of the aquifer: 328.88–611.96 mg/L for QU, 236.00–571.19 mg/L for QL, 299.71–2,127.66 mg/L for P, and 855.48–1,986.61 for O2. For domestic consumption and irrigation, a TDS <1,000 mg/L is required, which was found in QU and QL. The TH of groundwater varied from 18.92 to 1,371.81 mg/L: 158.84–336.43 mg/L for QU, 86.92–221.65 mg/L for QL, 18.92–193.30 mg/L for P, and 557.84–1,371.81 mg/L for O2, meaning that in QU and QL, the water ranged from soft (TH <150 mg/L) to slightly hard (TH within 150–300 mg/L) according to the classification of Chinese Standards for Drinking Water Quality (GB5749-2006). Soft water may be due to recharge from local precipitation, or surface-water bodies with low concentrations of Ca^{2+} and Mg^{2+} .

For all samples, the major cations and anions showed broad ranges: Na^+ = 4.34–560.45, Ca^{2+} = 1.36–371.17, Mg^{2+} = 0.33–139.23, Cl^- = 7.84–179.34, SO_4 = 2.26–1,178.61, and HCO_3 = 32.92–1,045.88 mg/L. The predominant cation and anion trends in QU were $\text{Ca}^{2+} > \text{Na}^+ > \text{Mg}^{2+}$, and $\text{HCO}_3^- > \text{SO}_4^{2-} \approx \text{Cl}^-$. In QL and P, the ion trends were $\text{Na}^+ > \text{Ca}^{2+} > \text{Mg}^{2+}$, and $\text{HCO}_3^- > \text{SO}_4^{2-} > \text{Cl}^-$, suggesting that the lower Quaternary is hydraulically connected with the Permian aquifer. The trend of dominant ions in O2 were $\text{Ca}^{2+} > \text{Mg}^{2+} > \text{Na}^+$, and $\text{SO}_4^{2-} > \text{HCO}_3^- > \text{Cl}^-$. The dissolution of calcite and dolomite may be the result of relatively high concentrations of HCO_3^- , Ca^{2+} and Mg^{2+} , while the high concentration of SO_4^{2-} in O2 may be from the dissolution of gypsum.

From the hydrogeological perspective, as shown in Table 1 and Fig. 3, 18 of 72 water samples were classified. Na^+ was recorded as “ $\text{Na}^+ + \text{K}^+$ ” because the concentration of K^+ was low in this area. For these water samples, there were four main groundwater chemical types: Na- HCO_3 in P, Ca- HCO_3 in QU, Na-Ca- HCO_3 in QL, and Ca- SO_4 in O2, indicating that the

three main aquifers in this study area have relatively independent hydrogeochemical conditions. Na-HCO₃ and Ca-Mg-SO₄-HCO₃ were the dominant water chemical types in T, while the surface pit lake was classified as Ca-Mg-HCO₃-SO₄. The Permian aquifer is above coal seam No. 3, and almost all of the sampled tunnel water was from P. However, some tunnel water samples were collected when the underground Ordovician borehole carried out the drainage tests, as well as one surface pit water sample, making these samples dominated by Ca-Mg-SO₄-HCO₃.

Figure 3 shows that QU samples are located where the carbonate hardness exceeds 50%, which means that the total hardness of most water samples can be decreased using water softening techniques. Permian water samples are located in areas dominated by alkaline earth and weak acids. Ordovician samples plot in the area where strong acids exceed weak acids and noncarbonate hardness exceeds 50%. QL water samples are distributed in a relatively dispersed pattern. As time progressed and mining techniques advanced and changed, the dominant cation in QL evolved from calcium to sodium (Fig. 3, shown by the black arrow), and the dominant anion changed from chloride to bicarbonate. As the QL provides recharge for the Ordovician limestone aquifer, the concentrations of groundwater ions from QL into O2 increase or decrease due to mineral dissolution along different flow paths. It can be derived from the hydrogeochemical facies that the concentrations of ions in groundwater in the four

dominant aquifers affected by mining activity is controlled by the dissolution/precipitation of calcite, dolomite, gypsum, and Na-containing minerals such as halite and albite. Small amounts of nitrite and ammonia were also detected in the water samples, indicating that these samples showed different levels of contamination according to the Chinese Standards for Drinking Water Quality (GB5749-2006).

Multivariate statistical analysis

Figure 3 shows the classification of all the water samples. R-mode HCA was performed on all samples in conjunction with Ward's linkage method with squared Euclidean distance in order to measure the similarity between the water chemical variables. Results from the R-mode HCA are shown in Fig. 4, showing four major groups out of seven water chemical variables. Cluster 1 includes SO₄²⁻, Mg²⁺, and Ca²⁺, indicating carbonate dissolution. Cluster 2 is comprised of Na⁺ and HCO₃⁻, suggesting both carbonate dissolution and ion exchange. As discussed above, natural processes dominate the evolution of groundwater hydrogeochemistry in this case study.

Pearson correlation analysis was employed to interpret the correlations of the main ions, TDS, TH, and pH (Table 2). TH was significantly correlated with TDS (0.716), Ca²⁺ (0.990) and Mg²⁺ (0.977), while TDS was also significantly correlated with Ca²⁺ and Mg²⁺, making Ca²⁺ and Mg²⁺ the major

Fig. 3 Piper diagram of all water samples

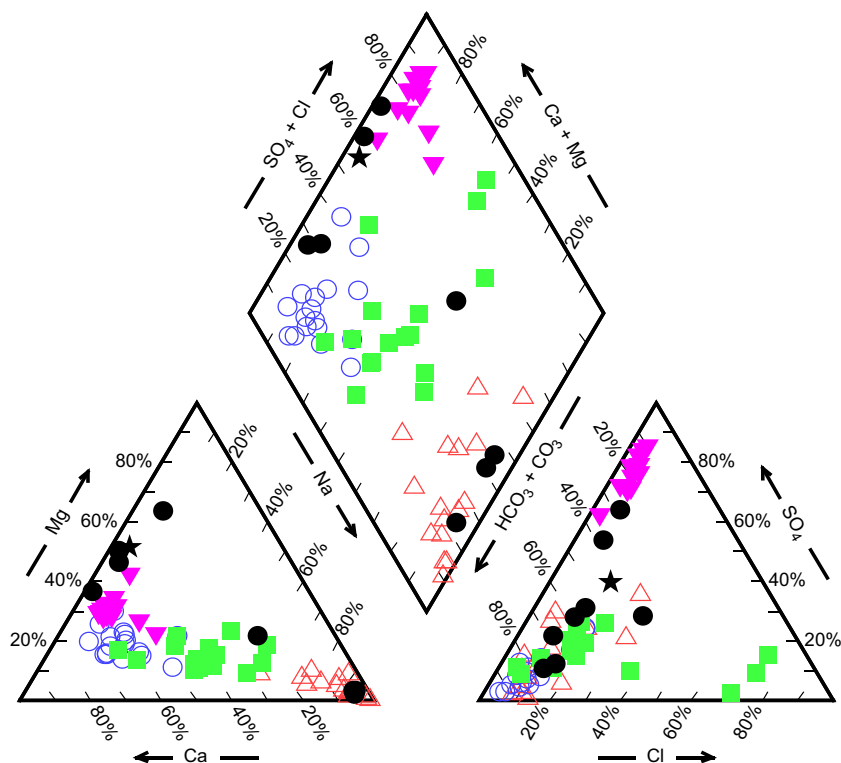
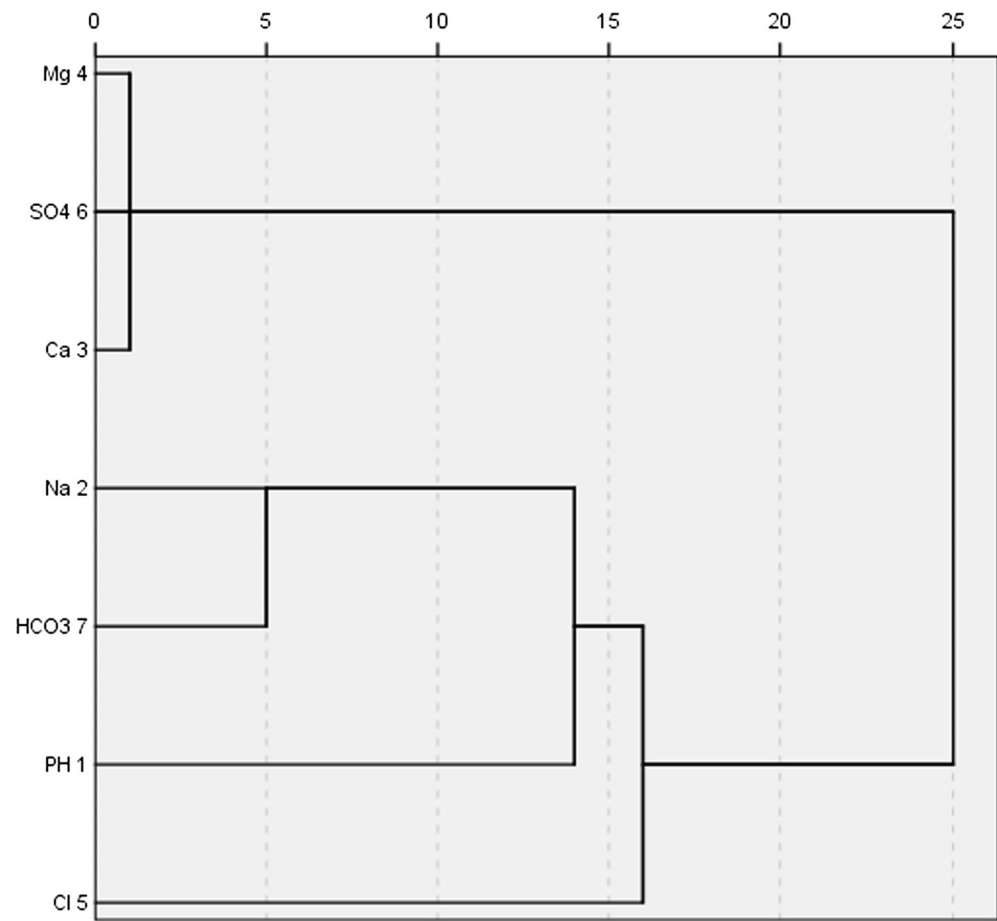


Fig. 4 Dendrogram of HCA results

contributors to TH. In addition, Na^+ was correlated with HCO_3^- (0.864) instead of Cl^- , indicating that groundwater chemistry is dominated by the contribution from ion exchange rather than halite and albite dissolution. Ca^{2+} (0.951) and Mg^{2+} (0.969) were significantly correlated with SO_4^{2-} , which means that in the Ordovician aquifer, the groundwater chemistry is dependent on the dissolution of gypsum, oxidation of pyrite, and ion exchange.

Based on the Kaiser criterion, PCA provided two significant principle components (PCs), as shown in Table 3. The eigenvalues for the first two PCs contributed 73.95% of the observed variance, and the contribution of PC1 was larger than PC2. Table 4 and Fig. 5 show the identified PCs. PC1 contained most of the main ions in the Ordovician aquifer (Ca^{2+} , Mg^{2+} , and SO_4^{2-}), which were also the dominant ions for TDS and TH, whereas PC2

Table 2 Correlation matrix of the species in all samples

Correlation	pH	Na^+	Ca^{2+}	Mg^{2+}	Cl^-	SO_4^{2-}	HCO_3^-	TDS	TH
pH	1.000	0.431	-0.407	-0.327	0.141	-0.275	0.299	-0.065	-0.383
Na^+		1.000	-0.334	-0.232	0.463	-0.085	<i>0.864</i>	0.437	-0.303
Ca^{2+}			1.000	<i>0.953</i>	-0.062	<i>0.951</i>	-0.294	<i>0.693</i>	<i>0.990</i>
Mg^{2+}				1.000	0.029	<i>0.969</i>	-0.240	<i>0.747</i>	<i>0.977</i>
Cl^-					1.000	0.076	0.114	0.249	-0.044
SO_4^{2-}						1.000	-0.134	<i>0.840</i>	<i>0.965</i>
HCO_3^-							1.000	0.409	-0.279
TDS								1.000	<i>0.716</i>
TH									1.000

Significant factors are in italic font

Table 3 Eigenvalues of the correlation matrix

PCs	Eigenvalue	Percentage of variance %	Cumulative %
1	<i>3.352</i>	<i>47.880</i>	<i>47.880</i>
2	<i>1.825</i>	<i>26.069</i>	<i>73.949</i>
3	0.826	11.799	85.748
4	0.701	10.019	95.767
5	0.239	3.414	99.182
6	0.044	0.628	99.810
7	0.013	.190	100.000

Significant factors are in italic font

consisted of Na^+ , HCO_3^- , Cl^- , and pH, which represents the main ions in QU, QL, and P. From Fig. 6, one can see that the QU and QL are similarly distributed and are more closely related to PC2, indicating that QU and QL share a similar hydrogeochemical environment. Permian water samples are also closer to PC2 and are generally larger than 0.4. The water samples from O2 are more closely related to PC1, but are dispersed along a wider range, meaning that the distances QL supplied to O2 were different. Two tunnel water samples are close to O2 because they were collected in the tunnel where the O2 boreholes were draining. Other tunnel water samples were more similar to the distributions of P, QU, and QL, suggesting that in daily mining operations, QU, QL, and especially P, are the main sources of drainage water into the mine.

Hydrogeochemical processes

The potential reactants for groundwater in this study area were carbonates (calcite and dolomite), crystal minerals (gypsum and quartz), and some clay minerals (kaolinite, illite and montmorillonite). The presence of pyrite and siderite may be disregarded, because the detected iron ion concentrations were too small to impact the hydrogeochemical environment. The study showed that the major reactants were calcite, dolomite,

Table 4 Eigenvectors of the two PCs

Species	Coefficient of PC1	Coefficients of PC2
SO_4^{2-}	<i>0.989</i>	0.028
Mg^{2+}	<i>0.976</i>	-0.094
Ca^{2+}	<i>0.954</i>	-0.231
Na^+	-0.134	<i>0.882</i>
HCO_3^-	-0.157	<i>0.819</i>
Cl^-	0.140	<i>0.596</i>
pH	-0.339	<i>0.542</i>

Significant factors are in italic font

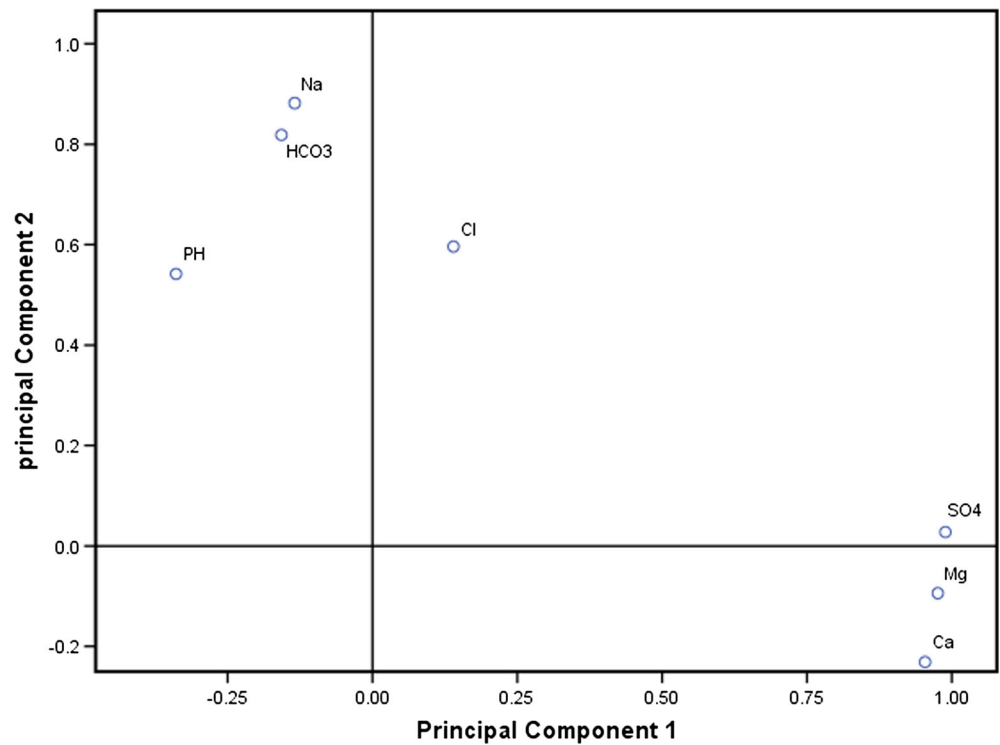
gypsum and halite, and clay minerals which implied that the cation exchange should be assessed.

The saturation index (SI) values for calcite and dolomite in the four main aquifers were mostly greater than zero (Table 1), suggesting that the two minerals are super-saturated and have the potential to precipitate. In contrast, the SI of gypsum in all four aquifers for all the samples was below zero, indicating that the gypsum is in a dissolved water environment. Groundwater in recharge areas is often undersaturated with respect to minerals, indicating the short distance of the flow path and time of interaction between water and rock. Generally, the value of TDS in an aquifer increases down the flow path due to extensive water–rock interactions and dissolution of minerals, suggesting that TDS could be used to verify runoff direction and other groundwater characteristics (Gastmans 2010).

The SI values of calcite and dolomite ranged from -0.16 to 0.64 and -2.27 to 0.83, respectively, in QU; from -0.64 to 0.84 and -1.57 to 1.32 in QL; -0.32 to 1.03 and -1.07 to 1.87 in P; and from 0.33 to 1.04 and 0.52 to 1.92 in O2, respectively. The SI values of calcite and dolomite in the QU, QL, and P aquifers were not correlated with TDS, as shown in Fig. 7. In contrast, in all four aquifers, $\text{SI}_{\text{Gypsum}}$ and TDS had relatively proportional correlations. $\text{SI}_{\text{Gypsum}}$ and $\text{SI}_{\text{Halite}}$ in all the water samples were less than zero, meaning that the groundwater had the capacity to dissolve gypsum and halite, and the resulting increased concentration of Ca^{2+} could induce the super-saturation of calcite and dolomite. Furthermore, the concentrations of Ca^{2+} , Mg^{2+} , and HCO_3^- were not strongly correlated with $\text{SI}_{\text{Calcite}}$ (Fig. 8a) and $\text{SI}_{\text{Dolomite}}$ (Fig. 8b), which suggests that the calcite and dolomite stopped dissolving. As shown in Fig. 8c, $\text{SI}_{\text{Gypsum}}$ increases with a polynomial fit along with the concentrations of Ca^{2+} and SO_4^{2-} . The correlation coefficients (R^2) of Ca^{2+} and $\text{SI}_{\text{Gypsum}}$, and SO_4^{2-} and $\text{SI}_{\text{Gypsum}}$ are 0.91 and 0.94, respectively.

Kumar (2009) employed the relationship between TDS and ions to reveal the mechanics of their hydrogeochemical evolution and to analyze the origin of the ions. Out of all the cations in the water samples, the rates of increase of Na^+ in P and Ca^{2+} and Mg^{2+} in O2 were greater than those for other cations in other aquifers, which showed insignificant correlations. The correlations between Na^+ and TDS in P, Ca^{2+} and TDS in O2, and Mg^{2+} and TDS in O2, were 0.90, 0.88, and 0.66, respectively (Fig. 9a). For anions, TDS and the concentration of SO_4^{2-} in O2 showed the highest correlation ($R^2 = 0.97$) in all the water samples. Also, HCO_3^- in P had a relatively large correlation of 0.82 (Fig. 9b), indicating that halite dissolution and cation exchange were the dominant hydrogeochemical processes in P.

Fig. 5 Loadings plot of PCs



As the gypsum dissolved in O₂, carbonate minerals became super-saturated and began to precipitate, causing HCO₃⁻ concentration to be in a lower range.

The dissolution of carbonate minerals could be denoted as Eqs. (1) and (2). If hydrogeochemistry of the groundwater consisted of ions coming solely from the dissolution of calcite, (HCO₃⁻)/(Ca²⁺) would be 2, whereas if the dissolution of

dolomite was the cause for the concentration of ions in the water, the ratio would be 4.

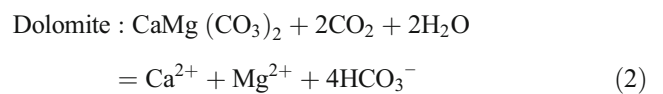
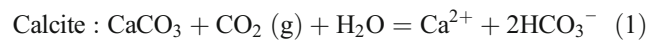
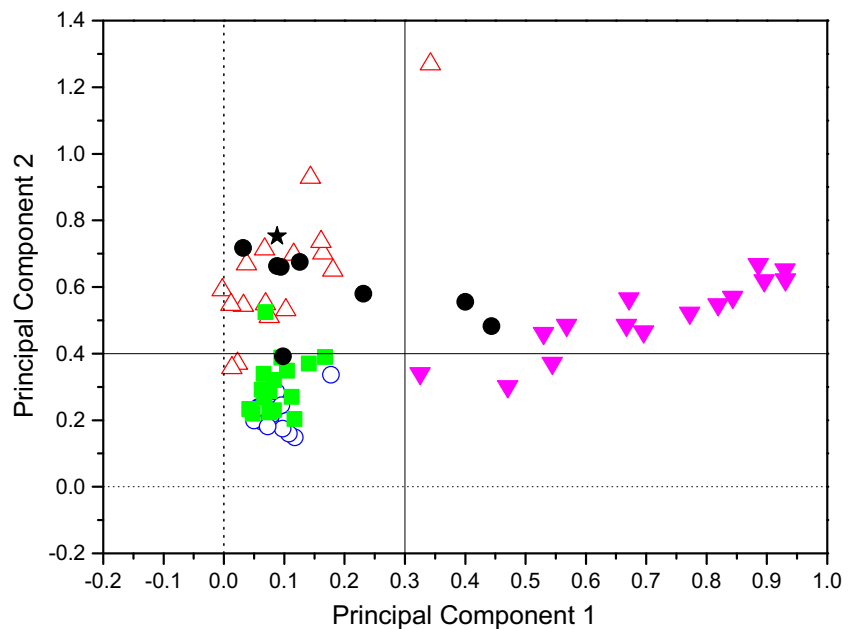


Fig. 6 Scores plot of PC1 and PC2



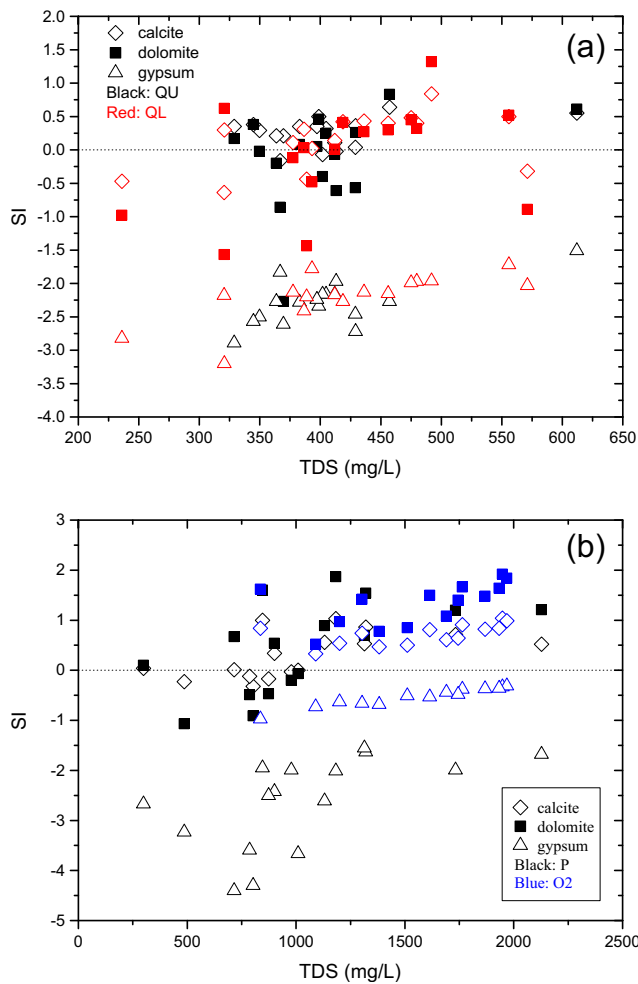


Fig. 7 Saturation index and TDS for **a** QU and QL, **b** Permian and Ordovician

Figure 10a shows the scatter plots of Ca^{2+} and HCO_3^- for the four main aquifers, whereby there are three zones in Fig. 10: under the 2:1 line, between the 2:1 and 4:1 lines, and above the 4:1 line. The zone under the 2:1 line represents a deficiency of HCO_3^- , and consists of 14 water samples from O2, three samples from QL and one from QU. The zone in the middle is a transition area, where the dissolution of both calcite and dolomite occurs or cation exchange consumes calcium ions. The zone above the 4:1 line must be accompanied by ion exchange. As shown in Fig. 10a, it is notable that QU and QL groundwater were more likely formed by calcite and dolomite dissolution. The Permian aquifer was characterized by cation exchange. As shown in Fig. 10b and Table 1, there is further evidence that the dissolution/precipitation of calcite and dolomite was the dominant hydrogeochemical process. From Fig. 10c, Ca^{2+} and SO_4^{2-} show a higher correlation. All the water samples are around the 1:1 line from Eq. (3), while O2 and most of P cluster

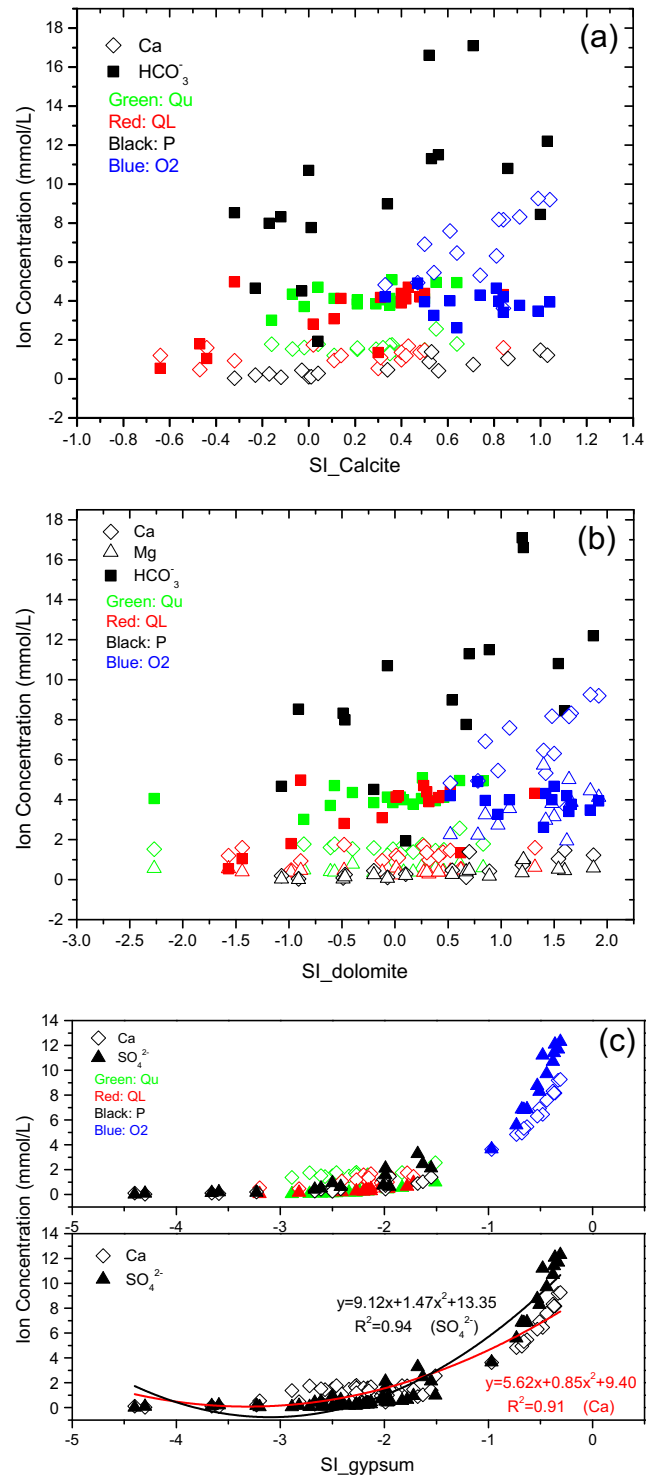
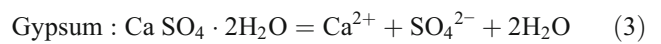


Fig. 8 **a** $\text{SI}_{\text{Calcite}}$ and ion concentration, **b** $\text{SI}_{\text{Dolomite}}$ and ion concentration, **c** $\text{SI}_{\text{Gypsum}}$ and ion concentration

above it, and QU and QL below it, indicating that O2 and P participate in cation exchange, and there may be reverse ion exchange in QU and QL.



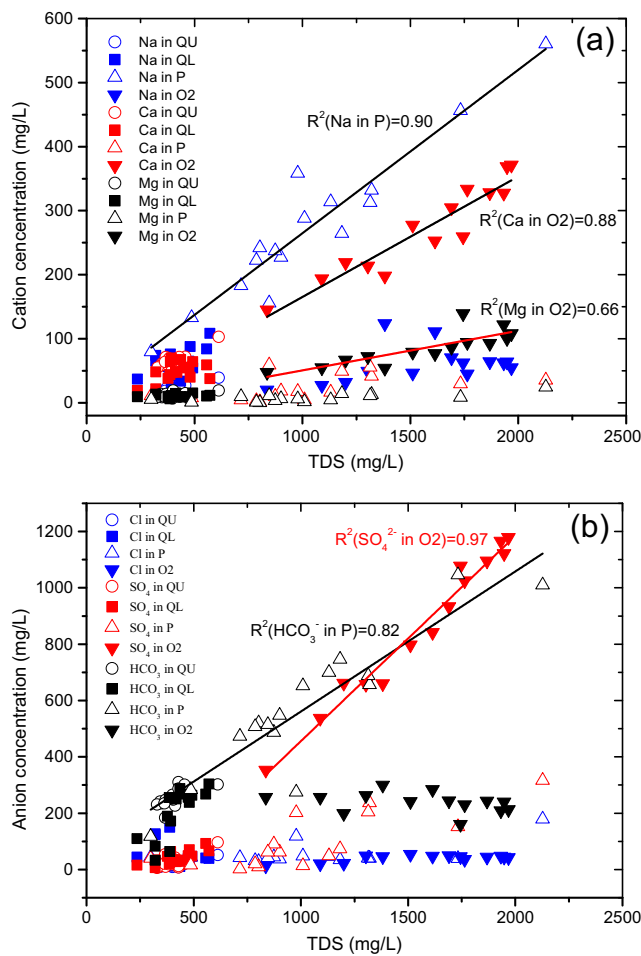


Fig. 9 a TDS and cation concentration, b TDS and anion concentration

If Ca^{2+} , Mg^{2+} , and Na^+ come from the dissolutions of their corresponding minerals (calcite, dolomite, and halite), the Na/Cl could be 1 (Rajmohan and Elango 2004; Ettazarini 2005). Figure 11 shows that all the water samples except three from P are below the 1:1 line. All the water samples have more halite ions than chloride ions, while the groundwater types are controlled by ion exchange. Figure 12 shows that Ca^{2+} and Mg^{2+} are both deficient compared with SO_4^{2-} and HCO_3^- . Because calcite dissolves faster than dolomite, it is assumed that calcium will be the major cation participating in ion exchange. As shown in Fig. 13, the samples in the upper left quadrant (including some from QU and QL) may represent reverse ion exchange, and other samples in the lower right quadrant are consistent with cation exchange. The groundwater from P has the strongest degree of ion exchange of the four aquifers. As shown in Eq. (4), the processes of adsorbing Ca^{2+} and desorbing Na^+ may be the main direction of the cation exchange. The exchange type of Eq. (4) can be verified by the chloro-alkaline indices (CAI-1 and CAI-2) proposed by Schoeller (1965).

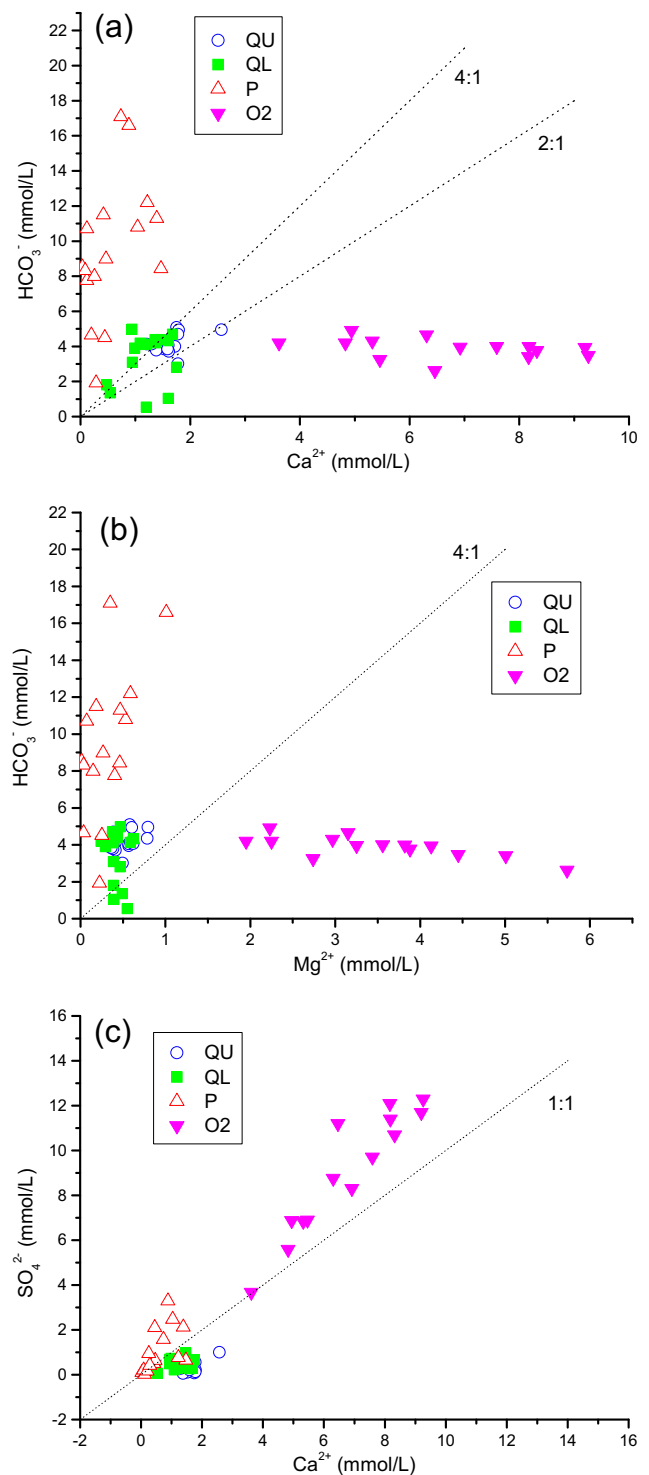
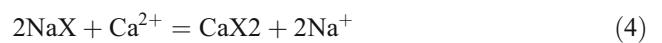


Fig. 10 a Ca and HCO_3^- concentration, b Mg and HCO_3^- concentration, c Ca and SO_4 concentration



As already discussed, results showed that water in P is in a hydrogeochemical environment that promotes strong ion exchange, inducing that calcium is at a much lower

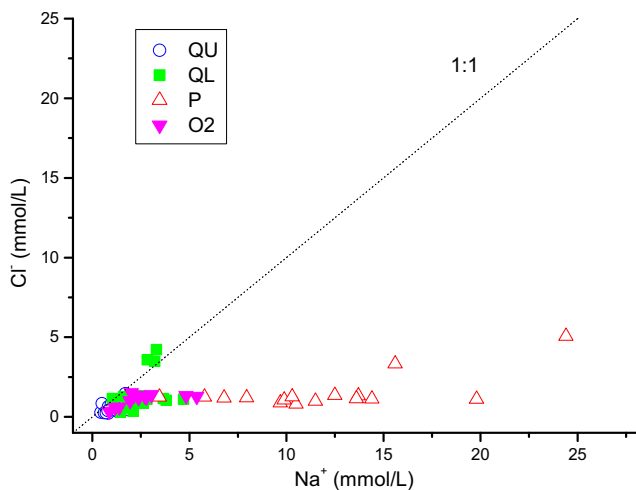


Fig. 11 Na and Cl concentration

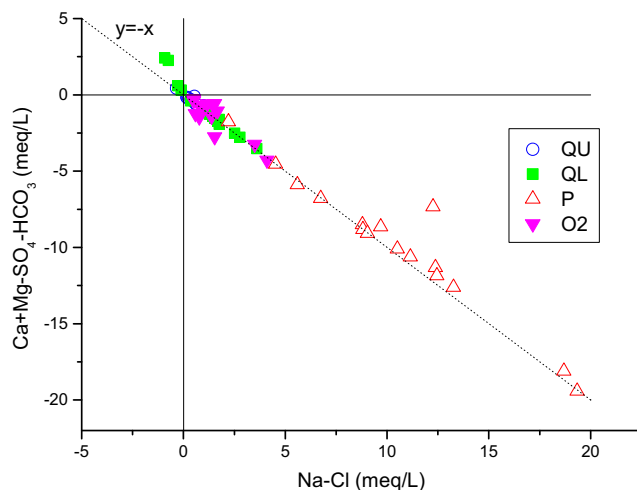


Fig. 13 Na-Cl and Ca+Mg-SO₄-HCO₃ concentration

concentration than bicarbonate. The dissolution of calcite and dolomite in O2 has ceased, indicating that the dominant dissolved mineral in O2 is gypsum. The four main aquifers have relatively independent hydrogeochemistry, although they have different piezometric heads, suggesting that the hydraulic conductivity of natural faults is weak and the sealing property of hydrogeological drilling in the coal field is good. Another possibility is that the deep coal seams Nos. 16 and 17 have not been extracted, so the faults were not activated by coal mining.

Since 1979, coal seam No. 3 has been the active mining layer in the Xinglongzhuang Coal Mine, and the Permian aquifer is the main water-inrush source. QL is the replenishment source for both the Permian and Ordovician aquifers, while at the same time, QL receives recharge from precipitation and QU (Fig. 14). Large areas of coal mining can cause the water level of QL to drop. QL is an unconsolidated, confined aquifer; due to coal mining and increasing drainage from the Permian aquifer,

the skeleton of QL would be compressed, potentially causing a change in hydrogeochemistry. QU has Ca-HCO₃ dominated water chemistry with calcite and dolomite as the dominant minerals, allowing ion exchange between Ca²⁺ and Na⁺ to occur. When water enters QL, cation exchange is the main hydrogeochemical process, producing a Na-Ca-HCO₃ water type. As QL is the recharge source for P, the water type in P is Na-HCO₃ as a result of the ion exchange in the source. An extended period of coal mining drained much of the water from P, which induced a decrease in water volume and in the water table of both P and QL. Mining caused the rock strata to sink, and obstructed the path connecting P and QL. All these reasons may have brought about a state of intensified ion exchange in QL. Figure 15 shows the changing concentrations of sodium and calcium in QL as the duration of mining activity increases. The increased Na⁺ and decreased Ca²⁺ trends over time could be used to verify the action of cation exchange.

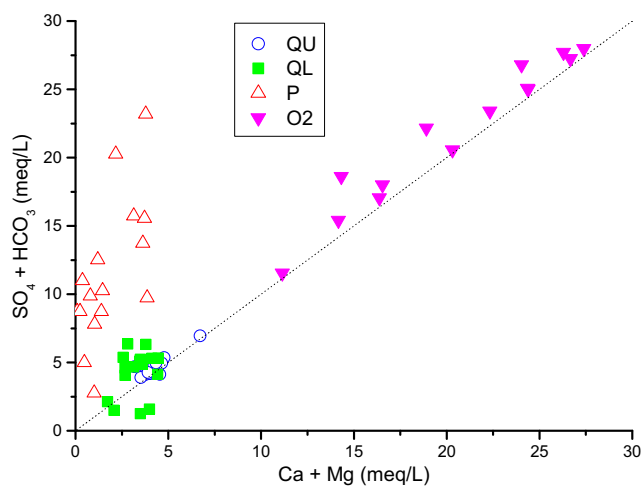


Fig. 12 Ca+Mg and SO₄+HCO₃ concentration

As shown in Fig. 16a, the water inflow (average annual value) at the Xinglongzhuang Coal Mine was in a relatively stable range, from a minimum of 52.84 m³/h in 1976 to a maximum of 297.62 m³/h in 2011, and an average value of 227.40 m³/h for all observed years. The precipitation in the study area fluctuated from minimum of 311.7 mm in 2002 to 1,050.5 mm in 2003 (Fig. 16b). Generally, wet and dry years alternated; however, there was not an obvious correlation between precipitation and water inflow. The upper Quaternary water table was shown to be above sea level (Fig. 16c), although its elevation has been decreasing over time with coal mining activity, from -17.53 m in 1983 to -89.22 m above sea level in 2012. Water-table data were collected on December 31st of every year. Coal mining activities directly used water from the Permian aquifer, which is recharged by the lower Quaternary aquifer. Currently,

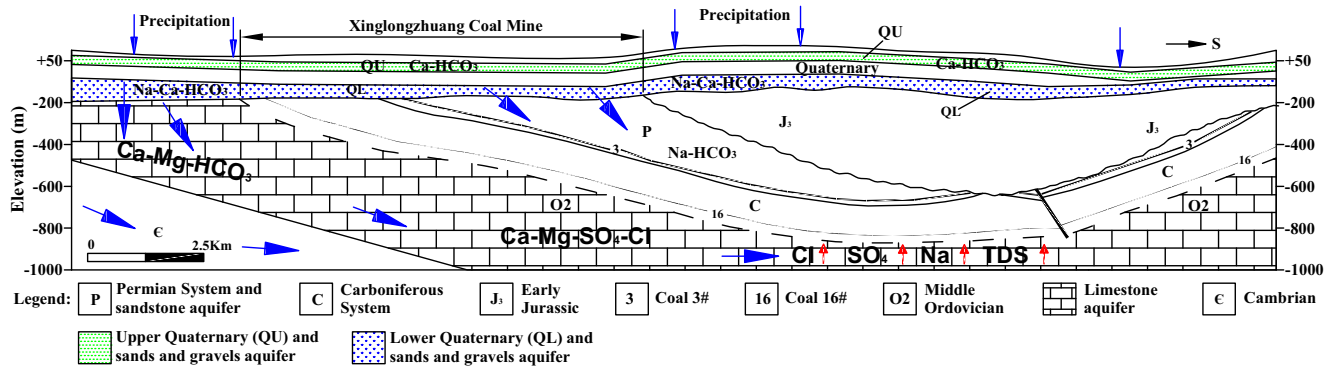


Fig. 14 Hydrogeological conceptual model

the water table of the Permian aquifer is around -200 m above sea level, meaning that the Permian and lower Quaternary aquifers have large static reserves; however, the recharge water volume for QL was smaller than the drainage, leading the water table to drop each year. The lack of adequate fresh water recharge in QL caused an increase (Na⁺) and decrease (Ca²⁺) in the related exchanging ions (Fig. 15).

Trace element analysis

Acid mine drainage (AMD) poses a severe pollution problem to current and future generations, and is a major problem at coal mines all over the world. Different concentrations of heavy metals are found naturally in groundwater, deposited by geological processes and biological cycles. Certain trace elements from mine drainage become toxic to humans and must be monitored. For this study, 26 heavy metals (Ge, As, Al, Ti, Ba, Tl, Pb, Th, U, Li, Be, Sc, V, Cr, Mn, Co, Ni, Cu, Zn, Ga, Rb, Sr, Zr, Mo, Cd and

Cs) were selected for monitoring, while five water samples were taken (T1, T2, T3, T4, and T5) for trace elements detection. Sample locations were dispersed throughout the mine: T1 was located in the panel and from the roof water, T2 and T3 were located at the end of ditch connected directly with the mine total sump, although T2, past the ditch, was from the roof water of the panel, and T3 was from an Ordovician exploration well, T4 was obtained from the total sump, and T5 was from the surface pit.

As shown in Table 5, the concentration of 26 trace metals in the five water samples was tested. Al, Ba, Li, Ni, Sr, and Mo were the dominant elements in the mine drainage. With the exception of Ni, most of these metals were below the allowable limit as provided in the standards of Ministry of Health of the P.R. of China (2006). Ni was below the 20 µg/L in T1–T4, but exceeded the drinking-water allowable limit in T5 (53.3 µg/L). There was cement and fly ash in the ditches, so that the concentration of trace elements in water samples was affected by the flowing environment. The concentration of Ti, Pb, Li, V, Co, Cu, Zn, and Mo gradually increased along the path of the flowing water. From the data in T1 and T2, one can see that the concentration of Ti, U, Be, Sc, Mn, Sr, Cd, and Cs has only a slight change; however, the concentration of Al, Ba, Th, Cr, Ga, Rb, and Zr increased as water flowed through the ditches. The concentration of Ba, Th, Sc, and Cr from the roof water decreased after it was mixed with Ordovician water. In the total sump, there was some simple hydrochemical treatment and precipitation, resulting in a decrease in the concentration of Ti, V, Mn, Ga, Sr, and Zr. Relatively high concentrations of Sr in the drainage may be attributed to the weathering of calcium carbonate minerals. Concentrations of most metals were below the acceptable limits, indicating that the highly alkaline pH could weaken the dissolution of metals, and that the clay minerals provide a good adsorbing surface for many trace elements. Some concentrations of ions in the drainage water were very high (Table 1), meaning that the drainage water is not suitable for drinking (WHO 2017). In the future, when coal seams Nos. 16 and 17 are extracted, the

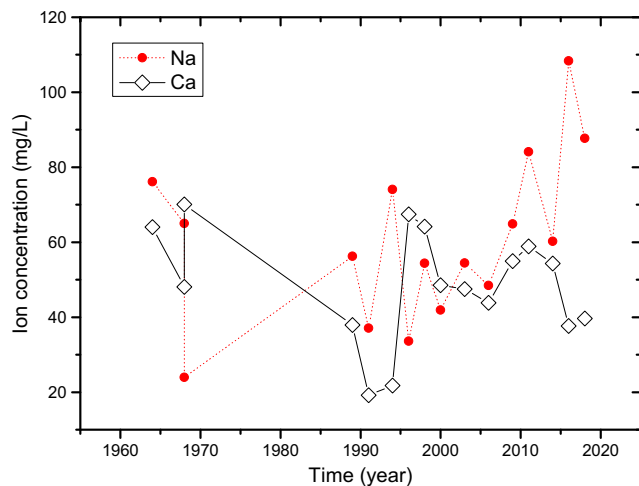


Fig. 15 Concentrations of Na and Ca along with time in groundwater of the upper Quaternary aquifer

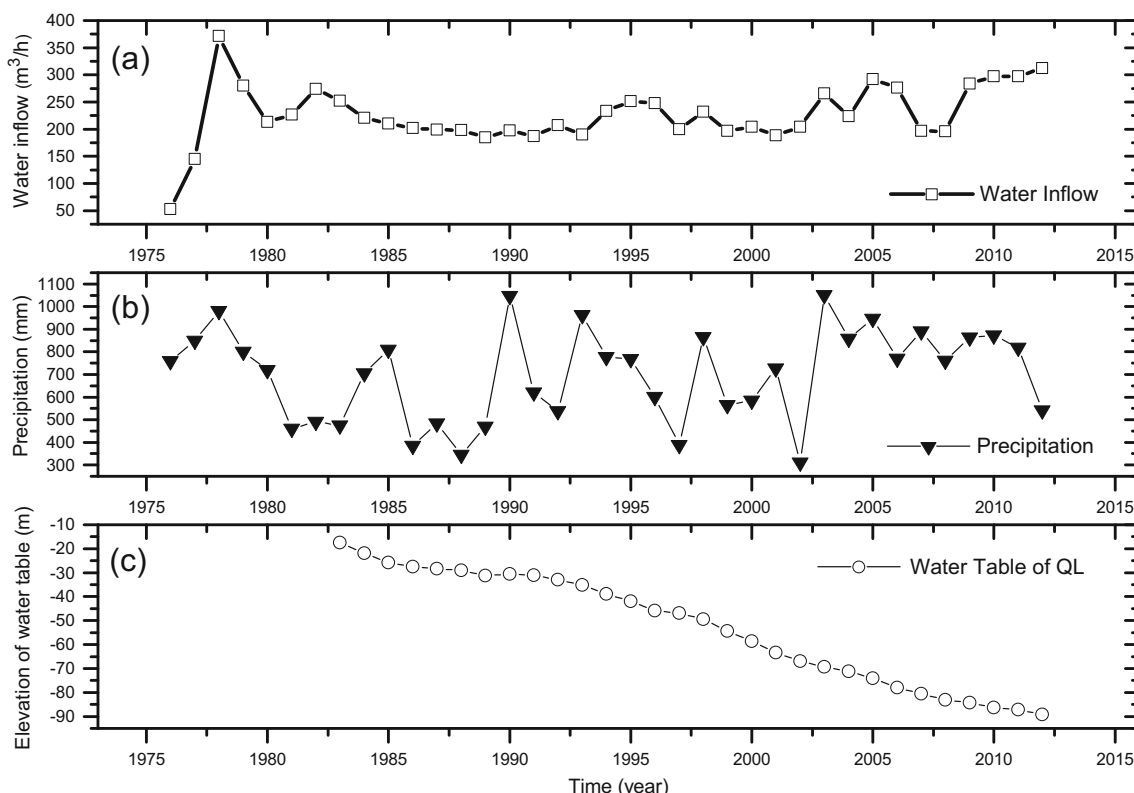


Fig. 16 a Water inflow, b precipitation, and c elevation of water table vs. time

Ordovician aquifer would be the main source of drainage water, and the high concentration of sulfates would be the main water treatment problem encountered when reusing the mine water.

Conclusions

This study investigated the trace elements in and evolution of the hydrogeochemistry of mine drainage water at the Xinglongzhuang Coal Mine in the Shandong Province of China using ion analysis, multivariate statistical techniques, and correlation analyses. The following conclusions can be summarized.

- Four main groundwater chemical types in the aquifers were identified: Na-HCO₃ in P, Ca-HCO₃ in QU, Na-Ca-HCO₃ in QL, and Ca-SO₄ in O2. The concentrations of ions in groundwater in the four dominant aquifers were influenced by the dissolution/precipitation of calcite, dolomite, gypsum, and Na containing minerals.
- The R-mode HCA analysis showed that the hydrogeochemical evolution in the study area was driven by carbonate dissolution and active ion exchange, and that natural processes dominated this evolution over time. PC1 contained most of the main ions in the Ordovician aquifer (Ca²⁺, Mg²⁺, and SO₄²⁻), which were also the dominant

Table 5 Trace element chemistry of Xinglongzhuang Coal Mine discharges

Trace element	Site number				
	T1	T2	T3	T4	T5
Ge (µg/L)	0.00	0.39	0.00	0.00	0.00
As (µg/L)	0.000	0.000	0.000	0.000	0.000
Al (µg/L)	0.031	0.048	0.035	0.033	0.059
Ti (µg/L)	0.007	0.004	0.019	0.015	0.008
Ba (µg/L)	127.0	161.0	71.4	77.3	102
Tl (µg/L)	0.014	0.017	0.024	0.028	0.032
Pb (µg/L)	0.067	0.088	0.080	0.082	0.924
Th (µg/L)	0.031	0.120	0.053	0.030	0.027
U (µg/L)	0.35	0.31	0.18	0.32	0.18
Li (µg/L)	11.5	67.9	90.8	73.1	133.0
Be (µg/L)	0.003	0.002	0.003	0.001	0.002
Sc (µg/L)	3.23	3.13	2.80	2.91	2.40
V (µg/L)	0.85	1.51	1.63	1.64	2.46
Cr (µg/L)	4.39	11.5	3.04	4.94	8.58
Mn (µg/L)	6.52	0.84	4.00	3.62	0.66
Co (µg/L)	0.11	0.15	1.17	1.49	9.27
Ni (µg/L)	1.07	1.18	8.34	9.69	53.3
Cu (µg/L)	2.58	7.57	2.83	4.76	11.0
Zn (µg/L)	1.01	1.26	2.18	3.97	14.5
Ga (µg/L)	0.007	0.084	0.086	0.070	0.047
Rb (µg/L)	1.87	4.05	13.00	9.39	9.48
Sr (µg/L)	1848	1708	4591	3577	2277
Zr (µg/L)	0.084	0.55	0.11	0.18	0.067
Mo (µg/L)	1.52	1.38	4.85	7.20	27.90
Cd (µg/L)	0.008	0.005	0.009	0.016	0.063
Cs (µg/L)	0.017	0.089	0.28	0.15	0.15

contributors for TDS and TH. PC2 consisted of Na^+ , HCO_3^- , Cl^- , and pH, indicating the main ions in QU, QL, and P.

- The concentrations of sodium and calcium in QL varied with the length of time that the area was mined, meaning that gradually, the increase of Na^+ and decrease of Ca^{2+} could be used to verify the action of cation exchange. The Permian aquifer provides a hydrogeochemical environment that encourages strong ion exchange, and calcium was at a much lower concentration than bicarbonate. The dominant dissolution mineral in O2 was gypsum. The four main aquifers have relatively independent hydrogeochemistry, although they have different piezometric heads, suggesting that the hydraulic conductivity of natural faults is weak.
- Large spatial extents of coal mining can cause the water level of the four aquifers to drop. The flow path of the water combined with the water–rock interactions caused there to be different concentrations of ions, and therefore drove the ion exchange in groundwater.
- The concentrations of Ti, Pb, Li, V, Co, Cu, Zn, and Mo gradually increased along the flow path of the water. Concentrations of most metals were detected below the acceptable limits, indicating that a high alkaline pH could weaken the dissolution of metals, and that the presence of clay minerals provided a good adsorbing surface for many of the trace elements.
- Due to the limited number of water samples available from the study area, the overall understanding of groundwater evolution may be limited. In the future, when coal seam No. 16 is extracted, the Ordovician aquifer would be the main source of drainage water, and the high concentration of sulfate would be the main water treatment problem encountered when reusing the mine water.

Acknowledgements The authors thank the reviewers for their helpful comments.

Funding information The research was supported by the National Natural Science of China (Grant 41772302), the Fundamental Research Funds for the Central Universities (2017XKZD07), the Fundamental Research Funds for the Central Universities (2015QNB23), the Fundamental Research Funds of the State Key Program of National Natural Science of China (Grant 41430643), the State 973 Project (Grant 2015CB251601), and the Priority Academic Program Development of Jiangsu Higher Education Institutions.

References

- Adam PJ, Paul LY (2000) Broadening the scope of mine water environmental impact assessment: a UK perspective. *Environ Impact Assess Rev* 20:85–96. [https://doi.org/10.1016/S0195-9255\(99\)00032-3](https://doi.org/10.1016/S0195-9255(99)00032-3)
- Andreas K, Nikola R (2011) Special issue: sustainable development of energy, water and environment systems. *Water Resour Manage* 25: 2917. <https://doi.org/10.1007/s11269-011-9888-9>
- Babita N, Abhay KS, Pathak DD, Aaditya C (2017) Hydrogeochemistry of coal mine water of North Karanpura coalfields, India: implication for solute acquisition processes, dissolved fluxes and water quality assessment. *Environ Earth Sci* 76:489. <https://doi.org/10.1007/s12665-017-6813-4>
- Bhattacharya P, Sracek O, Eldvall B, Asklund R, Barmen G, Jacks G, Koku J, Gustafsson JE, Singh N, Balfors BB (2012) Hydrogeochemical study on the contamination of water resources in a part of Tarkwa mining area, western Ghana. *J Afr Earth Sci* 66–67:72–84. <https://doi.org/10.1016/j.jafrearsci.2012.03.005>
- Blake S, Henry T, Murray J, Flood R, Muller MR, Jones AG, Rath V (2015) Compositional multivariate statistical analysis of thermal groundwater provenance: a hydrogeochemical case study from Ireland. *Appl Geochem* 75:171–188. <https://doi.org/10.1016/j.apgeochem.2016.05.008>
- Carucci V, Petitta M, Aravena R (2012) Interaction between shallow and deep aquifers in the Tivoli Plain (central Italy) enhanced by groundwater extraction: a multi-isotope approach and geochemical modeling. *Appl Geochem* 27(1):266–280. <https://doi.org/10.1016/j.apgeochem.2011.11.007>
- Chen LW, Yin XX, Gui HR (2013) Water–rock interactions tracing and analysis of deep aquifers in mining area using isotope and hydrogeochemistry methods. *Acta Geol Sin* 8(7):1021–1030
- Chihhi H, Marsily GD, Belayouni H, Yahyaoui H (2015) Relationship between tectonic structures and hydrogeochemical compartmentalization in aquifers: example of the “Jeffara de Medenine” system, south-east Tunisia. *J Hydrol* 4:410–430. <https://doi.org/10.1016/j.ejrh.2015.07.004>
- Cortes JE, Muñoz LF, Gonzalez CA, Niño JE, Polo A, Suspes A, Siachoque SC, Hernández A, Trujillo H (2016) Hydrogeochemistry of the formation waters in the San Francisco field, UMV basin, Colombia: a multivariate statistical approach. *J Hydrol* 539:113–124. <https://doi.org/10.1016/j.jhydrol.2016.05.010>
- Ettazarini S (2005) Processes of water–rock interaction in the Turonian aquifer of OumEr-Rabia Basin, Morocco. *Environ Geol* 49(2):293–299. <https://doi.org/10.1007/s00254-005-0088-x>
- Gastmans D, Chang HK, Hutcheon I (2010) Groundwater geochemical evolution in the northern portion of the Guarani Aquifer System (Brazil) and its relationship to diagenetic features. *Appl Geochem* 25(1):16–33. <https://doi.org/10.1016/j.apgeochem.2009.09.024>
- Güler C, Thyne GD, McCray JE, Turner KA (2002) Evaluation of graphical and multivariate statistical methods for classification of water chemistry data. *Hydrogeol J* 10(4):455–474. <https://doi.org/10.1007/s10040-002-0196-6>
- Guo HM, Wang YX (2003) Hydro-geochemical processes in shallow Quaternary aquifers from the northern part of Datong Basin, China. *Appl Geochem* 19(1):19–27. [https://doi.org/10.1016/S0883-2927\(03\)00128-8](https://doi.org/10.1016/S0883-2927(03)00128-8)
- Han Y, Wang GC, Cravotta CA, Hu WY, Bian YY, Zhang ZW, Liu YY (2013) Hydrogeochemical evolution of Ordovician limestone groundwater in Yanzhou, North China. *Hydrolo Proc* 27(16): 2247–2257. <https://doi.org/10.1002/hyp.9297>
- Huang X, Deng H, Zheng C, Cao G (2016) Hydrogeochemical signatures and evolution of groundwater impacted by the Bayan Obo tailing pond in northwest China. *Sci Total Environ* 543(Pt A):357–372. <https://doi.org/10.1016/j.scitotenv.2015.10.150>
- Johnson KL, Younger PL (2006) The co-treatment of sewage and mine waters in aerobic wetlands. *Eng Geol* 85(1–2):53–61. <https://doi.org/10.1016/j.enggeo.2005.09.026>
- Kumar SK, Rammohan V, Sahayam JD, Jeevanandam M (2009) Assessment of groundwater quality and hydrogeochemistry of Manimuktha River basin, Tamil Nadu, India. *Environ Monitor Assess* 159(1–4):341–351. <https://doi.org/10.1007/s10661-008-0633-7>
- Li PY, Feng W, Xue CY, Tian R, Wang S (2017) Spatiotemporal variability of contaminants in lake water and their risks to human health: a

- case study of the Shahu Lake tourist area, northwest China. *ExpoHealth* 9(3):213–225. <https://doi.org/10.1007/s12403-016-0237-3>
- Li PY, Tian R, Liu R (2018) Solute geochemistry and multivariate analysis of water quality in the Guohua Phosphorite Mine, Guizhou Province, China. *Exposure Health*. <https://doi.org/10.1007/s12403-018-0277-y>
- Ministry of Health of the P. R. China, Standardization Administration of the P. R. China (2006) Standards for drinking water quality (GB 5749-2006) (in Chinese). China Standard Press, Beijing
- Morán-Ramírez J, Ledesma-Ruiz R, Mählknecht J, Ramos-Leal JA (2016) Rock–water interactions and pollution processes in the volcanic aquifer system of Guadalajara, Mexico, using inverse geochemical modeling. *Appl Geochem* 68:79–94. <https://doi.org/10.1016/j.apgeochem.2016.03.008>
- Plummer LN, Busby JF, Lee RW (1990) Geochemical modeling of the Madison aquifer in parts of Montana, Wyoming, and South Dakota. *Water Resour* 26:1981–2014. <https://doi.org/10.1029/WR026i009p01981>
- Qiao W, Li WP, Li T, Chang JY, Wang QQ (2017) Effects of coal mining on shallow water resources in semiarid regions: a case study in the Shennan Mining Area, Shaanxi, China. *Mine Water Environ* 36:104–113. <https://doi.org/10.1007/s10230-016-0414-4>
- Rajmohan N, Elango L (2004) Identification and evolution of hydrogeochemical processes in the groundwater environment in an area of the Palar and Cheyyar river basins, southern India. *Environ Geol* 46(1):47–61. <https://doi.org/10.1007/s00254-004-1012-5>
- Rakotondrabe F, Ngoupayou JRN, Mfonka Z, Rasolomanana EH, Abolo AJN, Ako AA (2018) Water quality assessment in the Bétaré-Oya gold mining area (East-Cameroon): multivariate statistical analysis approach. *Sci Total Environ* 610–611:831–844. <https://doi.org/10.1016/j.scitotenv.2017.08.080>
- Razowska L (2001) Changes of groundwater chemistry caused by the flooding of iron mines (Czestochowa Region, southern Poland). *J Hydrol* 24:17–32. [https://doi.org/10.1016/S0022-1694\(00\)00420-0](https://doi.org/10.1016/S0022-1694(00)00420-0)
- Sako A, Bamba O, Gordio A (2016) Hydrogeochemical processes controlling groundwater quality around Bomboré gold mineralized zone, central Burkina Faso. *J Geochem Explor* 170:58–71. <https://doi.org/10.1016/j.gexplo.2016.08.009>
- Salmi EF, Nazem M, Karakus M (2017) Numerical analysis of a large landslide induced by coal mining subsidence. *Eng Geol* 217:141–152. <https://doi.org/10.1016/j.enggeo.2016.12.021>
- Schoeller H (1965) Qualitative evaluation of groundwater resources. In: *Methods and techniques of groundwater investigation and development*. Water Research, Series-33. UNESCO, Delft, The Netherlands, pp 54–83
- Sharif MU, Davis RK, Steele KF, Kim B, Kresse TM, Fazio JA (2008) Inverse geochemical modeling of groundwater evolution with emphasis on arsenic in the Mississippi River Valley alluvial aquifer, Arkansas (USA). *J Hydrol* 350(1–2):41–55. <https://doi.org/10.1016/j.jhydrol.2007.11.027>
- Towfiqul Islam ARM, Shen SH, Bodrud-Doza MD, Safiur Rahman M (2017) Assessing irrigation water quality in Faridpur district of Bangladesh using several indices and statistical approaches. *Arabian J Geosci* 10:418. <https://doi.org/10.1007/s12517-017-3199-2>
- Unlu T, Akcin H, Yilmaz O (2013) An integrated approach for the prediction of subsidence for coal mining basins. *Eng Geol* 166:186–203. <https://doi.org/10.1016/j.enggeo.2013.07.014>
- Voutsis N, Kelepertzis E, Tziritis E, Kelepertzis A (2015) Assessing the hydrogeochemistry of groundwaters in ophiolite areas of Euboea Island, Greece, using multivariate statistical methods. *J Geochem Explor* 159:79–92. <https://doi.org/10.1016/j.gexplo.2015.08.007>
- WHO (2017) Guidelines for drinking-water quality, fourth edition: incorporating the first addendum. World Health Organization, Geneva
- Wu Q, Fan ZL, Zhang ZW, Zhou WF (2014) Evaluation and zoning of groundwater hazards in Pingshuo no. 1 underground coal mine, Shanxi Province, China. *Hydrogeol J* 22:1693–1705. <https://doi.org/10.1007/s10040-014-1138-9>
- Zhang JC (2005) Investigations of water inrushes from aquifers under coal seams. *Int J Rock Mech Min Sci* 42:350–360. <https://doi.org/10.1016/j.ijrmm.2004.11.010>